ОБЪЕДИНЕННЫЙ
ИНСТИТУТ
ЯДЕРНЫХ
ИССЛЕДОВАНИЙ

Дубна

40-19

D1-2019-40

I. N. Meshkov [1,2,*]

# LUMINOSITY OF AN ION COLLIDER

Submitted to "Particles and Nuclei"

345

[1] Joint Institute for Nuclear Research, Dubna
[2] Saint Petersburg State University, Saint Petersburg, Russia
* E-mail: meshkov@jinr.ru

## INTRODUCTION

The problem of collider luminosity calculations has been known since the first proposals of colliding-beam accelerators*. As yet, nobody has come out with a sufficiently compact formula that describes the collider luminosity in the general case of collision of two beams with arbitrary parameters and allows analytical or numerical calculations to be performed without using mathematical modeling methods.

The work on the NICA project at the Joint Institute for Nuclear Research [1] required collisions of different ion beams, including those with different types of beam particles or different beam structure, e.g., collision of a bunched beam with a coasting beam, etc. This is how the asymmetric collider came into being. It turned out that no convenient formulas for analytical calculations of luminosity of these colliders could be found in the literature, including various reviews. They usually offered classical formulas suitable only for symmetric colliders with beams having identical parameters and differing, perhaps, only by the electric charge of the beam particles — electron–positron and proton–antiproton colliders [2, 3]. Sometimes, simplified formulas are given [4, 5], which do not involve the so-called "hourglass parameter" (Sec. 1.2 below).

Attempts to derive a formula for a rather general case usually lead to cumbersome expressions with multiple integrals over six coordinates of the coordinate–momentum space [6].

The need for this kind of formula persists despite highly developed methods for numerical modeling of particle dynamics in charged-particle accelerators. This formula is needed for carrying out calculations at the level of estimates, which is necessary for selecting initial collider parameters.

Section 1 of this work is an extended version of [7]. The case under consideration is a collision of two beams whose parameters (type of colliding particles,

---

*The first formula for estimation of luminosity was proposed by D. Kerst in his report presented in 1956 (*Kerst D. W.* Properties of an Intersecting-Beam Accelerating System // Proc. Intern. Conf. on High Energy Accel., Geneva, 1956. P. 37): the number of events per unit time for processes with the cross section in collisions of two bunches with the number of particles $N_1$ and $N_2$ and length $l$ at the particle velocity $v$ is $n = 2N_1 N_2 vlA$.

their number in the beam (bunch), and their energy) can be different, as also can be the size and shape of the collider rings, etc. Detailed consideration is given to the version of the collider in which axes of the colliding beams coincide in the interaction region ("head-on collisions") so that the beams can have common final-focus lenses. The version of the collider with intersecting beams is briefly presented. The "unavoidable" misprints made in the original version are corrected.

Section 2 describes a method for optimizing parameters of a cyclic collider by minimizing betatron frequency shifts caused by the action of the beam space charge. The author's first attempt (not quite successful) of this publication was made in [8]. The recently obtained refined version of the formula for the beam–beam effect is used.

Section 3 contains numerical examples of luminosity calculations for a few types of symmetric and asymmetric colliders, including the "equilibrium"-beam collider [9], which is of interest for modern nuclear physics.

The results are applicable to both counter-propagating and merging beams.

All luminosity formulas and their numerical values are given for one interaction point (IP) of a collider.

## 1. ASYMMETRIC COLLIDING BEAMS

**1.1. Luminosity: General Case.** The density distribution of the particles of a bunched beam, Gaussian in all three dimensions ($x$, $y$, $s$), has the form

$$\rho_i(t) = \frac{N_i}{(2\pi)^{3/2}\,\sigma_{xi}(t)\,\sigma_{yi}(t)\,\sigma_{si}} \exp\left\{-\frac{1}{2}\left(\frac{x^2}{\sigma_{xi}^2(t)} + \frac{y^2}{\sigma_{yi}^2(t)} + \frac{s^2}{\sigma_{si}^2}\right)\right\}. \tag{1.1}$$

Here $N_i$ is the number of particles in a bunch of the $i$th beam; $i = 1, 2$ is the beam number; and $\sigma_{\alpha i}$ is the Gaussian parameter of the bunch of the $\alpha$-degree of freedom of the beam ($\alpha = x, y, s$). A similar density distribution formula for a coasting beam with the uniform density distribution over the circumference of the ring and the number of particles $N_i$ is

$$\rho_i(t) = \frac{N_i}{2\pi\sigma_{xi}(t)\,\sigma_{yi}(t)\,C_{\text{ring}}} \exp\left\{-\frac{1}{2}\left(\frac{x^2}{\sigma_{xi}^2(t)} + \frac{y^2}{\sigma_{yi}^2(t)}\right)\right\}. \tag{1.2}$$

To simplify the description of the collision kinematics (Fig. 1), we choose the time reference and the origin of coordinates so that at $t = 0$ the centers of both bunches are at the origin of coordinates ($x = y = s = 0$): $s_1^0(0) = s_2^0(0) = 0$.

This means that the collision time $t$ is

$$-\infty < t = \frac{s_1}{v_1} < \infty.$$



The coordinates of the bunch centers $s_i^0$ vary with time as

$$s_i^0(t) = v_i t, \quad x_i^0 = y_i^0 = 0. \tag{1.3}$$

We restrict ourselves to the case of the so-called head-on collisions, when the axes of the bunches coincide with each other and with the $s$ axis (Fig. 1). We also need the coordinates of the colliding particles $\eta_i$ measured from the centers of their bunches (in the laboratory system!). Then the $s_i$ coordinate of the $i$th particle in the laboratory system is (Fig. 1)

$$s_i(t) = s_i^0(t) + \eta_i. \tag{1.4}$$

The transverse coordinates of the particle are still measured from the $s$ axis in the laboratory system. The time dependence of the transverse sizes of the bunches $\sigma_{xi}(t)$, $\sigma_{yi}(t)$ arises from their motion in the focusing system

$$\sigma_{\alpha i}(t) = \sqrt{\varepsilon_{\alpha i} B_{\alpha i}(s_i(t))}, \quad \alpha = x, y, \quad i = 1, 2, \tag{1.5}$$

where $\varepsilon_{\alpha i} =$ const is the beam emittance,

$$B_{\alpha i}(s_i(t)) = B_{\alpha i}^* + \frac{s_i^2(t)}{B_{\alpha i}^*} \tag{1.6}$$

is the betatron (beta) function of the focusing system, $B_{\alpha i}^*$ is its minimum value usually achieved at the interaction point (IP) $s = 0$, and $s_i(t)$ is the coordinate of the particle at the time $t$.

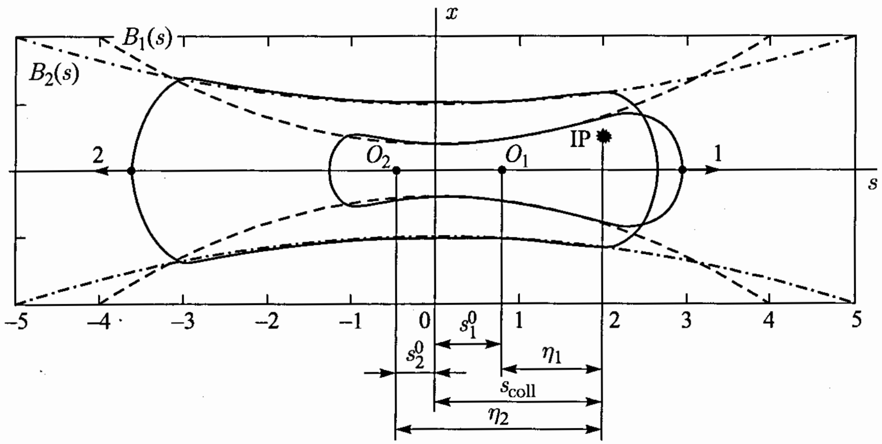


Fig. 1. Collision scheme of two bunches in the $y = 0$ plane. $O_{1,2}$ are the centers of the bunches; $\eta_{1,2}$ are the distances of the interaction point (IP) of two particles from the centers of the bunches; $s_{\text{coll}}$ is the same, from the origin; $B_{1,2}(s)$ are the envelopes (beta functions) of the first and second beams

We also assume that dispersion in the beam interaction region is zero, which occurs in most cases.

Within the collision time of two bunches, the layer of the first-bunch particles $\rho_1(x, y, \eta_1, t)\, d\eta_1$ intersects bunch 2, colliding with the particle layer $\rho_2(x, y, \eta_2, t)\, d\eta_2$ at each point $s(t)$. The coordinates of this point $s(t)$, $s_i(t)$, $s_i^0(t)$, and $\eta_i(t)$ are related to one another by the equalities (Fig. 1)

$$s(t) = s_1(t) = s_1^0(t) + \eta_1 = s_2(t) = s_2^0(t) + \eta_2. \tag{1.7}$$

Now we can write down the "obvious" expression for the luminosity at one IP:

$$L = n_{\text{bunch}} f_0 \int_{-\infty}^{\infty} dx \int_{-\infty}^{\infty} dy \int_{-l_D}^{l_D} d\eta_1 \int_{-l_D}^{l_D} d\eta_2 \rho_1(x, y, \eta_1(t)) \rho_2(x, y, \eta_2(t)), \tag{1.8}$$

where $n_{\text{bunch}} = \min\{n_{\text{bunch1}}, n_{\text{bunch2}}\}$ is the smallest number of bunches in beams 1 and 2, and $f_0$ is the rotation frequency of the particles of the beam with the smallest number of bunches. This choice of the $n_{\text{bunch}}$ and $f_0$ values follows from the collision synchronization condition (Sec. 1.5). Integrals over the longitudinal coordinates $\eta_1$ and $\eta_2$ are approximately taken in finite terms with the values $\pm l_D$ defined below in the comments on formula (1.11).

Considering conditions (1.3) and (1.4), from equalities (1.7) follows the relation between the coordinates $\eta_1$ and $\eta_2$:

$$\eta_2(t) = \eta_1 + \left(1 - \frac{v_2}{v_1}\right) s_1^0(t).$$

Here $v_{1,2}$ are the algebraic values for the velocities of particles 1 and 2.

Introducing the designations $s_0(t) \equiv s_1^0(t)$, $\eta \equiv \eta_1$, we write

$$\eta_2 = \eta + V s_0, \quad V \equiv 1 - \frac{v_1}{v_2}. \tag{1.9}$$

The parameter $V \geqslant 1$ is for counter-propagating colliding beams, and $V \leqslant 1$ is for merging beams.

Since we introduced the variable $s_0(t) = v_1 t$ and expressed $\eta_2$ in terms of $\eta$ and $s_0$, integration over the collision time in (1.8) can be replaced by integration over $s_0$ (the coordinate of the center of the first bunch), and integration over the bunch lengths can be replaced by integration over the variable $\eta$. The variable replacement Jacobian is

$$\frac{D(\eta_1, \eta_2)}{D(s_0, \eta)} = V. \tag{1.10}$$



As a result, we arrive at the expression

$$L = \frac{n_{\text{bunch}} N_1 N_2 f_0}{(2\pi)^3 \sigma_{s1} \sigma_{s2}} V \int_{-l_D}^{l_D} ds_0 \int_{-\infty}^{\infty} d\eta \int_{-\infty}^{\infty} \psi_x(x)\, dx \int_{-\infty}^{\infty} \psi_y(y)\, dy \times \exp\left[-\frac{1}{2}\left(\frac{\eta^2}{\sigma_{s1}^2} + \frac{(\eta + V s_0)^2}{\sigma_{s2}^2}\right)\right], \tag{1.11}$$

where

$$\psi_x(x, s_0, \eta_1) = \frac{1}{\sigma_{x1}(s_0, \eta)\, \sigma_{x2}(s_0, \eta)} \times \exp\left[-\left(\frac{1}{\sigma_{x1}^2(s_0, \eta)} + \frac{1}{\sigma_{x2}^2(s_0, \eta)}\right) \frac{x^2}{2}\right], \tag{1.12}$$

and $2l_D$ is the longitudinal ($s$) size of the region where the axes of both beams coincide and the detector is located. Local luminosity at $s_0 = \pm l_D$ decreases by a few orders of magnitude from the maximum value at $s_0 = 0$ due to increasing beta function, as is shown in Sec. 1.5.

The function $\psi_y(y,\ s_0,\ \eta_1)$ is found by replacing the subscript and the argument $x$ with $y$.

Integration of $\psi_x$ over $dx$ gives

$$\int_{-\infty}^{\infty} \psi_x(x, s_0, \eta_1)\, dx = \frac{\sqrt{2\pi}}{\sqrt{\sigma_{x1}^2(s_0, \eta) + \sigma_{x2}^2(s_0, \eta)}}. \tag{1.13}$$

The integral $\int_{-\infty}^{\infty} \psi_y(y, s_0, \eta_1)\, dy$ is similarly calculated by replacing $x$ with $y$.

Using values (1.5) for $\sigma_{xi}$, we write

$$\sqrt{\sigma_{x1}^2(s_0, \eta) + \sigma_{x2}^2(s_0, \eta)} = \sqrt{\varepsilon_{x1} B_{x1}(s_0, \eta) + \varepsilon_{x2} B_{x2}(s_0, \eta)}. \tag{1.14}$$

Functions $B_{xi}$ are defined in (1.6). A similar expression for $\sigma_{yi}$ is obtained by replacing $x$ with $y$.

Substituting values of integral (1.13) and denominator (1.14) as well as their $y$-analogues in (1.11), we arrive at quite a cumbersome expression for the luminosity of the collider with completely asymmetric bunches

$$L = \frac{n_{\text{bunch}} N_1 N_2 f_0}{(2\pi)^2 \sigma_{s1} \sigma_{s2}} V \int\limits_{-l_D}^{l_D} ds_0 \int\limits_{-\infty}^{\infty} d\eta \times$$

$$\times \frac{\exp\left\{-\frac{1}{2}\left[\frac{\eta^2}{\sigma_{s1}^2} + \left(\frac{\eta + V s_0}{\sigma_{s2}}\right)^2\right]\right\}}{\sqrt{\left(\varepsilon_{x1} B_{x1}(s_0, \eta) + \varepsilon_{x2} B_{x2}(s_0, \eta)\right)\left(\varepsilon_{y1} B_{y1}(s_0, \eta) + \varepsilon_{y2} B_{y2}(s_0, \eta)\right)}}. \tag{1.15}$$

Note that this is the collider luminosity at one IP. In addition, beta functions at IPs have different values $(B_{x,y})_{1,2}$ if particles 1 and 2 differ in at least one parameter — charge, mass, or energy. Therefore, we can introduce the "parameter of relative magnetic rigidity" $\lambda$:

$$\lambda = \frac{B_1^*}{B_2^*}. \tag{1.16}$$

Since the betatron functions $B_{1,2}$ are proportional to the magnetic rigidity of the colliding particles (similar to focal lengths of magnetic lenses), it can be expected that the parameter $\lambda$ is described by the expression

$$\lambda = \frac{p_1}{Z_1} \frac{Z_2}{p_2}. \tag{1.17}$$

Here $Z_{1,2}$ and $p_{1,2}$ are the charge and the momentum of the particles of beams 1 and 2. At equal velocities of particles 1 and 2, expression (1.17) does not depend on the particle velocity and is

$$\lambda_0 = \frac{m_2}{m_1} \frac{A_1}{Z_1} \frac{Z_2}{A_2},$$

where $A_{1,2}$ are the atomic weights of the particles, and $m_{1,2}$ are the masses of the nucleons of colliding particles 1 and 2 (difference of $m_2/m_1$ from unity is less than $1 \cdot 10^{-3}$ for all nuclei of the Periodic Table). However, values of $\lambda$ (1.17) and $\lambda_0$ are approximate, since the beta function in the common region of the rings is greatly affected by the parameters of the focusing systems in the individual sections.

With beams of different particles, we also have $\lambda = 1$ if in their common (interaction) region the focusing systems of two collider rings do not have focusing elements that govern the beta functions of the collider rings. This takes place, for example, in colliders with intersecting rings (Sec. 1.6).

Expression (1.15) is substantially simplified in three particular cases considered below.



**1.2. Identical Colliding Beams.** For identical counter-propagating colliding beams we have

$$\begin{gathered} v_1 = -v_2, \quad V = 2, \quad B_{x1}^* = B_{x2}^* \equiv B_x^*, \quad B_{y1}^* = B_{y2}^* \equiv B_y^*, \\ \sigma_{s1} = \sigma_{s2} \equiv \sigma_s, \quad \varepsilon_{x1} = \varepsilon_{x2} \equiv \varepsilon_x, \quad \varepsilon_{y1} = \varepsilon_{y2} \equiv \varepsilon_y. \end{gathered} \tag{1.18}$$

Taking into account the values of $B_{\alpha i}$ (1.6) and $\eta$ (1.9), from (1.15) we obtain

$$L = \frac{n_{\text{bunch}} N_1 N_2 f_0}{8\pi^2 \sigma_s^2 \sqrt{\varepsilon_x \varepsilon_y B_x^* B_y^*}} \times \text{Int}_1\left(B_x, B_y, \sigma_s\right),$$

$$\text{Int}_1 = 2 \int\limits_{-l_D}^{l_D} ds_0 \int\limits_{-\infty}^{\infty} d\eta \frac{1}{\sqrt{\left[1 + \left(\frac{s_0 + \eta}{B_x^*}\right)^2\right]\left[1 + \left(\frac{s_0 + \eta}{B_y^*}\right)^2\right]}} \times$$

$$\times \exp\left[-\frac{\eta^2 + (\eta + 2s_0)^2}{2\sigma_s^2}\right].$$

Transforming the numerator of the exponent index

$$\eta^2 + (\eta + 2s_0)^2 = 2\left[(s_0 + \eta)^2 + s_0^2\right],$$

going from the integration variables $s_0$ and $\eta$ to the variables $s_0$ and $\phi = s_0 + \eta$, and calculating the transition Jacobian $D(s_0, \eta)/D(s_0, \phi) = 1$, we obtain

$$\text{Int}_1 = 2 \int\limits_{-l_D}^{l_D} e^{-s_0^2 \sigma_s^2} ds_0 \int\limits_{-\infty}^{\infty} \frac{e^{-\phi^2/\sigma_s^2}}{\sqrt{\left[1 + \left(\frac{\phi}{B_y^*}\right)^2\right]\left[1 + \left(\frac{\phi}{B_x^*}\right)^2\right]}} d\phi.$$

Thus, the double integral is transformed to a product of two integrals. When $\sigma_s \ll l_D$, the first of them, the integral over $s_0$, is $\sigma_s\sqrt{\pi}$. When $B_x^* = B_y^* \equiv B^*$, we obtain the known expression for the luminosity of a collider with axially symmetric beams (see [2], formulas (6.134), (6.135))

$$L = \frac{n_{\text{bunch}} N_1 N_2 f_0}{4\pi\sqrt{\varepsilon_x \varepsilon_y} B^*} \Phi_{\text{HG}}, \quad \Phi_{\text{HG}}(\alpha) = \frac{2}{\sqrt{\pi}} \int\limits_0^{\infty} \frac{e^{-u^2} du}{1 + (\alpha u)^2}, \quad \alpha = \frac{\sigma_s}{B^*}. \tag{1.19}$$

Here $\Phi_{\text{HG}}(\alpha)$ is the hourglass parameter describing luminosity dependence on $\sigma_s$ and $B^*$.

**1.3. Collision of the Coasting Beam with the Bunched Beam.** As before, we consider the focusing system axially symmetric in the interaction region, but now the beams have particles of different types and differ, generally speaking, by energy. Therefore,

$$B_{x1}^* = B_{y1}^* \equiv B_1^* \neq B_{x2}^* = B_{y2}^* \equiv B_2^*. \tag{1.20}$$

The luminosity formula for the case where one of the colliding beams ($N_2$) is a coasting beam with uniform density (1.2) over the ring circumference $C_{\text{ring}}$ differs from (1.15) by the expression in the denominator of the fraction in front of the integral, which is now $(2\pi)^{3/2}\sigma_s C_{\text{ring}}$. Here $\sigma_s \equiv \sigma_{s1}$ is the "Gaussian" length of the beam bunch.

For axially symmetric beams, formula (1.15) takes the form

$$L = \frac{n_{\text{bunch}} N_1 N_2 f_0}{(2\pi)^{3/2}\sigma_s C_{\text{ring}}} \times \text{Int}_2\left(B_1, B_2, \sigma_s\right),$$

$$\text{Int}_2 = V \int_{-l_D}^{l_D} ds_0 \int_{-l_D}^{l_D} d\eta \times$$

$$\times \frac{1}{\varepsilon_1 B_1^*\left[1 + \left(\dfrac{s_0+\eta}{B_1^*}\right)^2\right] + \varepsilon_2 B_2^*\left[1 + \left(\dfrac{s_0+\eta}{B_2^*}\right)^2\right]} \exp\left\{-\frac{\eta^2}{2\sigma_s^2}\right\}. \tag{1.21}$$

Here $n_{\text{bunch}}$ and $f_0$ are the number of bunches in the bunched beam and the rotation frequency of its particles. Generally speaking, the parameter $V$ can differ from 2.

Let us transform variables in the same way as above,

$$\phi = s_0 + \eta, \qquad \psi = \eta.$$

The transition Jacobian is $D(s_0, \eta)/D(\phi, \psi) = 1$. As a result, integral (1.21) is divided into two independent integrals:

$$\text{Int}_2 = V \int_{-l_D}^{l_D} \exp\left(-\frac{\psi^2}{2\sigma_s^2}\right) d\psi \int_{-2l_D}^{2l_D} \frac{d\phi}{\varepsilon_1 B_1^*\left[1 + \left(\dfrac{\phi}{B_1^*}\right)^2\right] + \varepsilon_2 B_2^*\left[1 + \left(\dfrac{\phi}{B_2^*}\right)^2\right]}.$$

Integrating, we obtain

$$L = \frac{n_{\text{bunch}} N_1 N_2 f_0}{2\pi C_{\text{ring}}} V \operatorname{erf}\left(\frac{l_D}{\sqrt{2}\sigma_s}\right) \times$$

$$\times \sqrt{\frac{B_1^* B_2^*}{(\varepsilon_1 B_1^* + \varepsilon_2 B_2^*)(\varepsilon_1 B_2^* + \varepsilon_2 B_1^*)}}\, 2\arctan\left(\chi_D\right), \tag{1.22}$$



$$\chi_D = \sqrt{\frac{\varepsilon_1 B_2^* + \varepsilon_2 B_1^*}{\varepsilon_1 B_1^* + \varepsilon_2 B_2^*}}\, \frac{2l_D}{\sqrt{B_1^* B_2^*}}.$$

Under the condition that

$$\sigma_s,\ B_{1,2}^* \ll l_D \ll C_{\text{ring}}, \quad \chi_D \gg 1, \tag{1.23}$$

expression (1.22) takes a more compact form

$$L = \frac{n_{\text{bunch}} N_1 N_2 f_0}{2C_{\text{ring}}} V \sqrt{\frac{B_1^* B_2^*}{(\varepsilon_1 B_1^* + \varepsilon_2 B_2^*)(\varepsilon_1 B_2^* + \varepsilon_2 B_1^*)}}. \tag{1.24}$$

Expression (1.24) can be simplified using parameter $\lambda$ (1.16):

$$L = \frac{n_{\text{bunch}} N_1 N_2 f_0}{2C_{\text{ring}}} V \sqrt{\frac{\lambda}{\lambda(\varepsilon_1^2 + \varepsilon_2^2) + \varepsilon_1\varepsilon_2(1+\lambda^2)}}. \tag{1.25}$$

And a very simple expression for the luminosity is obtained for the colliding beams with identical particles, energies, and emittances: $\lambda = 1$, $V = 2$, and $\varepsilon_1 = \varepsilon_2 \equiv \varepsilon$,

$$L = \frac{n_{\text{bunch}} N_1 N_2 f_0}{2C_{\text{ring}}\varepsilon}. \tag{1.26}$$

**1.4. Collision of Two Coasting Beams.** Under conditions (1.20) and $B_{1,2}^* \ll C_{1,2}$, in the way similar to (1.21), we obtain luminosity from (1.15),

$$L = \frac{N_1 N_2 f_0}{2C_1 C_2} \times \text{Int}_3,$$

$$\text{Int}_3 = V \int_{-l_D}^{l_D} ds_0 \int_{-l_D}^{l_D} d\eta \frac{1}{\varepsilon_1 B_1^*\left[1 + \left(\dfrac{s_0+\eta}{B_1^*}\right)^2\right] + \varepsilon_2 B_2^*\left[1 + \left(\dfrac{s_0+\eta}{B_2^*}\right)^2\right]}.$$

Here $N_1$ and $N_2$ are the numbers of particles in beams 1 and 2, and $C_1$ and $C_2$ are the circumferences of the storage rings. The collision frequency is $f_0 = \max\{v_1/C_1, v_2/C_2\}$.

Integrating as in (1.21)–(1.25), we obtain

$$L = \frac{N_1 N_2 f_0}{\pi C_1 C_2} V l_D \sqrt{\frac{B_1^* B_2^*}{(\varepsilon_1 B_1^* + \varepsilon_2 B_2^*)(\varepsilon_1 B_2^* + \varepsilon_2 B_1^*)}}\, 2\arctan\left(\chi_D\right), \tag{1.27}$$

where the parameter $\chi_D$ is defined in (1.22). When $B_{1,2}^* \ll l_D$, $\chi_D \gg 1$, we obtain

$$L = \frac{N_1 N_2 f_0}{C_1 C_2} V l_D \sqrt{\frac{\lambda}{(\varepsilon_1\lambda + \varepsilon_2)(\varepsilon_1 + \varepsilon_2\lambda)}}. \tag{1.28}$$

For identical collider rings and colliding beams, there is $V = 2$ and $\lambda = 1$, and formula (1.28) takes the form

$$L = \frac{N^2 f_0}{C^2 \varepsilon}\, l_D. \tag{1.29}$$

**1.5. Distribution of Luminosity over the Interaction Region Length.** Modulation of collider beta functions (1.6) near the IP inevitably leads to luminosity variation along the interaction region length. It is most simply demonstrated for identical colliding beams (Sec. 1.2). Indeed, the derivative of the luminosity with respect to the coordinate $s_0$ is proportional to the integrand function in the expression for $\Phi_{\mathrm{HG}}(\alpha)$ in (1.19):

$$\frac{dL}{ds_0} = \left(\frac{dL}{ds_0}\right)_{\max} \frac{\mathrm{e}^{-(s_0/\sigma_s)^2}}{1 + \left(\dfrac{s_0}{B^*}\right)^2}.$$

Introducing the variable $\chi = s_0/B^*$, we obtain the luminosity distribution function normalized to the maximum

$$f_L(\chi) = \frac{\mathrm{e}^{-(\chi/\alpha)^2}}{1+\chi^2}, \quad \alpha = \frac{\sigma_s}{B^*}. \tag{1.30}$$

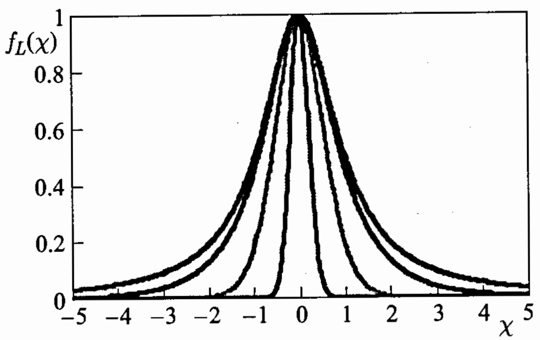


Fig. 2. Functions (1.30) of the luminosity distribution over the beam interaction region: $\alpha = 10; 3; 1; 0.3$

The graphs of this function (Fig. 2) show that as $\sigma_s$ (parameter $\alpha$) increases, the luminosity distribution function broadens until its width reaches saturation ($\chi > 5$).

This saturation corresponds to the collision of two coasting beams (Sec. 1.4). In addition, the results presented in Fig. 2 allow choosing

$$l_D = 3B^*. \tag{1.31}$$

**1.6. Collision of Intersecting Beams.** To increase luminosity in modern colliders, a multibunch regime is used, which usually implies that there are two independent rings to avoid parasitic collisions in the common regions of the trajectories and collision of beams at an angle. This is called "intersecting beams". Outside the interaction region, the beams are separated far enough, so that their focusing systems do not have common elements, which allows independently adjusting parameters of two colliding beams in an asymmetric collider. This is especially important for the electron–ion collider (Sec. 3.3).



The longitudinal axes of the focusing systems of two rings govern the axes of the colliding beams, while their local beta functions are still described by relations (1.6) but in the "intrinsic" coordinates of the rings $x_{\alpha i}$, whose axes $s_i$ intersect at the IP at the angle of $2\theta$ ("full crossing angle") (Fig. 3). The rings are arranged so that all three axes $s_1$, $s_2$, and $s_0$ lie in the same plane. The axes $y_i$ also lie in this plane, and the axes $x_i$ coincide and are orthogonal to the $(s_i, y_i)$ plane. The directions of the axes are not chosen at random: this choice ensures the fastest separation of the beams, which is needed if $\sigma_{xi} \geqslant \sigma_{yi}$.

The efficiency of beam separation in the interaction region is usually estimated by the ratio between the $y$ coordinate of the point on the bunch axis as far as $\sigma_s$ from the IP ($\delta y_0 = \sigma_s \sin\theta$, Fig. 3) and the projection of the transverse size of the bunch $\sigma_y$ on the $y_0$ axis ($\Delta y_0 = \sigma_y \cos\theta$). This parameter is referred to as the Piwinski angle

$$\phi = \frac{\sigma_s}{\sigma_y}\tan\theta. \tag{1.32}$$

The length of the interaction region (colored grey in Fig. 3) $2l_D$ can be estimated as

$$l_\theta = \frac{\sigma_x}{\sin\theta}, \quad \sigma_x \ll \sigma_s. \tag{1.33}$$

In the general case, it is

$$l_\phi = \frac{\sigma_s}{\sqrt{1+\phi^2}}. \tag{1.34}$$

Note that for $\phi \gg 1$ and $\theta \ll 1$, formula (1.34) coincides with (1.33), and for $\phi \ll 1$, $l_D \approx \sigma_s$.

In colliders with intersecting beams, the angle $\theta \ll 1$. For example, in the LHC the angle $\theta$ referred to as the half crossing angle varies from 0.6 $\mu$rad to 0.32 mrad depending on the chosen collider regime and the experimental requirements [10], and in the KEKB it is 11 mrad [11]. Therefore, to estimate the luminosity of a collider with intersecting beams, one can use the above

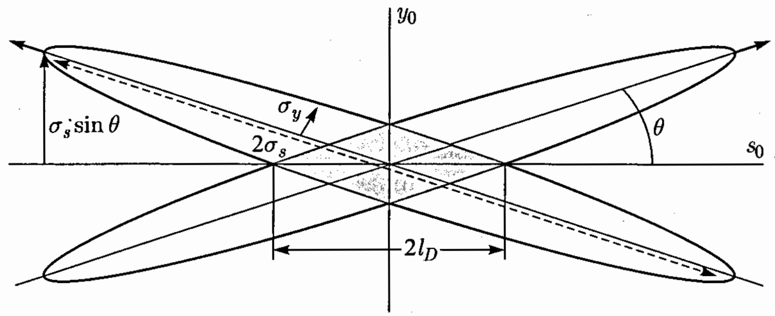


Fig. 3. Collision scheme of intersecting beams for $\phi \gg 1$; the oval boundaries show the "1 sigma sizes"; colored grey is the particle interaction region

formulas (Secs. 1.1–1.4), replacing $\sigma_y$ with $\sigma_y\sqrt{1+\phi^2}$ and using formulas (1.33) and (1.34) for $l_D$.

Nevertheless, the scheme of intersecting beams gives rise to two other undesirable effects for compensating which the so-called crab technique is used*.

The first effect is a nonzero collision angle $2\theta$ of two counter-propagating bunches. To eliminate it, the "crab crossing" scheme is used [12]. On the trajectories of each beam, upstream and downstream of the IP, RF cavities are installed, which are tuned to the mode with the transverse magnetic field that reverses its sign during the passage of the bunch and is zero during the passage of the center. As a result, the "head" and the "tail" get oppositely directed field kicks, and bunches rotate around the axis (in Fig. 3) and arrive at the IP in the phase with their axes directed towards each other. The cavities downstream of the IP restore the initial orientation of the bunches.

The purpose of this operation is to suppress synchrobetatron resonances (more exactly, violate their excitation condition), which arise from bunches colliding at an angle. Resonances, including those of lower orders, are due to correlation between the transverse coordinate of the particles in the system of the counter-propagating beam (that is, the transverse impact) and the longitudinal coordinate. They are eliminated using the crab crossing scheme.

The other effect is more complicated. When the betatron function is decreased (for increasing luminosity) to the size of the interaction region, nonlinear betatron resonances are excited due to interaction of the particle with the field of the counter-propagating bunch (see also the "beam–beam effect", Sec. 3.1). To eliminate this effect, P. Raimondi proposed a method called the "crab waist" [13–15]. Special sextupole lenses are mounted in both rings in front of and behind the IP so that betatron resonances arising from the beam–beam effect are suppressed.

Unfortunately, the crab crossing and crab waist methods are incompatible, and one has to choose that of the two which gives higher luminosity in a particular case. The crab technique is an excellent choice for electron–positron colliders but is not always suitable for ion colliders.

Treating the "crab technique" in more detail is beyond the scope of this paper (see, for example, [16]).

**1.7. Synchronization of Collisions.** An asymmetric collider with bunched colliding beams is the most complicated version in terms of synchronizing collisions of two bunches of the beams. Bunched beams collide in the same region, common for both rings, if the particle revolution frequency $f_{1,2}$ and the number of bunches in the beams $(n_{\rm bunch})_{1,2}$ satisfy the equality

$$n_1\, n_{\rm bunch1}\, f_1 = n_2\, n_{\rm bunch2}\, f_2, \qquad (1.35)$$

*The technique was named by analogy between the motion of a bunch between "crab" resonators and the motion of a crab, which is known to move sideways ("physicists joking").



where $n_{1,2}$ are integers. The optimal choices of the ring sizes and the particle energy are such that $n_1 = n_2 = 1$. In this case, the collision frequency is

$$f_{\rm coll} = n_{\rm bunch1}\, f_1 = n_{\rm bunch2}\, f_2. \qquad (1.36)$$

This is the parameter $n_{\rm bunch}\, f_0$ in the collision of two bunched beams (see (1.8), (1.11), (1.15), etc.). Synchronization condition (1.35) is only fulfilled for particular energies (velocities $v_1$, $v_2$) of the colliding particles

$$v_2 = v_1\, \frac{n_1\, n_{\rm bunch1}}{n_2\, n_{\rm bunch2}}\, \frac{C_2}{C_1}. \qquad (1.37)$$

Since the parameters $n_{1,2}$ and $n_{\rm bunch1,2}$ are integers, the minimum change in the particle energy can only occur stepwise with steps $\Delta n = 1$. Scanning with a smaller step requires special measures for changing the orbit length of one of the beams.

Given equal ring circumferences and equal numbers $n_1 = n_2$ and $n_{\rm bunch1} = n_{\rm bunch2}$, particle velocities should obviously be chosen equal, and scanning in velocity (but not in energy!) can be performed with arbitrary but equal steps. If one or both beams are coasting, this problem does not exist. The aforesaid is especially important for colliding beams of moderately relativistic particles, as, for example, in electron–positron colliders [17].

When a coasting beam collides with a bunched beam, we have $f_{\rm coll} = n_{\rm bunch} f_0$, where $n_{\rm bunch}$ and $f_0$ are the parameters of the bunched beam; and when two coasting beams collide, we have

$$f_{\rm coll} = \max\{f_1, f_2\},$$

where $f_{1,2}$ are the revolution frequencies of the particles of the first and second beams.

## 2. OPTIMIZATION OF THE CYCLIC COLLIDER LUMINOSITY

**2.1. Beam Space Charge Effects.** The problem of stable motion of charged particles in cyclic accelerators is quite well studied, and various methods are developed for suppressing the destructive effect of instabilities. Among the strongest and hardest-to-suppress instabilities are space charge effects, which lead to a frequency shift of the particle betatron oscillations under the action of the intrinsic electromagnetic field of the beam (Laslett effect) and the field of the counter-propagating beam in the collider (beam–beam effect). The method of choosing optimum beam parameters to minimize these two effects is considered in this section.

*Laslett Effect.* The charge density distribution of a Gaussian bunch of particles with charge $Ze$ is described in the laboratory system by the formula

$$\rho_Z(x,y,s) = Ze\rho(x,y,s). \tag{2.1}$$

Here $\rho(x,y,s)$ is the bunch particle density distribution (1.1). In what follows, we consider long bunches $\sigma_s \gg \sigma_x$, $\sigma_y$, for which the electric field of the Gaussian bunch having an elliptical cross section with the semiaxes $\sigma_x$ and $\sigma_y$ in the region $x \ll \sigma_x$ and $y \ll \sigma_y$ is described by the formula (see, for example, [18])

$$E_{x,y}(s) = \frac{2\rho_0(s)}{\sigma_x+\sigma_y} \times \begin{cases} \dfrac{x}{\sigma_x}, & x \text{ — component,} \\ \dfrac{y}{\sigma_y}, & y \text{ — component,} \end{cases} \qquad \rho_0(s) = \frac{ZeN}{\sqrt{2\pi}\sigma_s} e^{-s^2}/2\sigma_s^2. \tag{2.2}$$

The magnetic field of the bunch in the laboratory system is connected to the electric field by the known relation $\mathbf{B} = 1/c\,[\mathbf{v},\mathbf{E}]$. From here on, all vector quantities are bold printed; $\mathbf{v}$ is the bunch velocity along the $s$ axis.

The force exerted on the bunch particle by the bunch field is described by the expression

$$\mathbf{F} = Ze\left(\mathbf{E} + \frac{1}{c}[\mathbf{v},\mathbf{B}]\right) = Ze\left(\mathbf{E} - \beta^2\mathbf{E}_\perp\right), \tag{2.3}$$

$\beta = \mathrm{v}/c$, $c$ is the speed of light. The transverse component of the force $\mathbf{F}$ is

$$\mathbf{F}_\perp = \frac{Ze}{\gamma^2}\mathbf{E}_\perp, \quad \gamma = \left(1-\beta^2\right)^{-1/2}. \tag{2.4}$$

The equation of betatron oscillations of a particle with mass $M$ in the focusing system of the collider ring with allowance for the action of the bunch field on this particle is described by the expression

$$\gamma M\left[\frac{d^2x}{dt^2} + Q_x^2\omega_0^2 x\right] = \frac{ZeE_x}{\gamma^2}, \tag{2.5}$$

where $Q_x$ is the number of the particle betatron oscillations along the $x$ coordinate for one particle turn in the ring (betatron number), and $\omega_0$ is the revolution frequency. Let us introduce the betatron frequency shift $\Delta q_x\omega_0$ that appears under the action of the $x$-component of force $\mathbf{F}_\perp$ (2.4) and transform Eq. (2.5) into

$$\frac{d^2x}{dt^2} = -\left(Q_x^2\omega_0^2 x - \frac{ZeE_x}{\gamma^3 M}\right).$$

Then we express the right-hand side as $-(Q_x+\Delta q_x)^2\omega_0^2 x$. If $s \ll \sigma_s$, $\Delta q_x \ll Q_x$, from equality of two expressions we obtain

$$\Delta q_x \approx -\frac{ZeE_x}{2Q_x\gamma^3 M\omega_0^2 x} = -\frac{Z^2Nr_p}{\gamma^3 A\langle\sigma_x(\sigma_x+\sigma_y)\rangle}\frac{1}{Q_x\omega_0^2\sqrt{2\pi}\sigma_s}. \tag{2.6}$$



Here we used the equalities and the following notation: $N$ is the number of particles per bunch (or beam); $r_p = e^2/m_pc^2 = 1.535\cdot 10^{-16}$ cm is the classical proton (nucleon) radius; $m_p \approx 938$ MeV/$c^2$ is proton (nucleon) mass; and $A$ is the particle mass in atomic mass units. We also used equalities where $\langle B_x\rangle$ is the circumference-average $x$-beta function, and $\varepsilon_x$ is the $x$-emittance of the beam. Ultimately, we obtain (see also [19])*

$$\begin{aligned} \Delta q_x &= -\frac{Z^2Nr_pk_{\text{bunch}}\langle B_x\rangle}{2\pi\beta^2\gamma^3 A\langle\sigma_x(\sigma_x+\sigma_y)\rangle} = \\ &= \frac{Z^2Nr_p}{2\pi\beta^2\gamma^3 A}\frac{\sqrt{B_x}}{\sqrt{\varepsilon_x}(\sqrt{\varepsilon_x\langle B_x\rangle}+\sqrt{\varepsilon_y\langle B_y\rangle})}k_{\text{bunch}}; \\ k_{\text{bunch}} &\equiv \frac{C_{\text{ring}}}{\sqrt{2\pi}\sigma_s}; \end{aligned} \tag{2.7}$$

$\Delta q_y$ is found using the replacement $x \leftrightarrow y$.

At $B_x = B_y$ and $\varepsilon_x = \varepsilon_y = \varepsilon$, we arrive at the classical Laslett formula [20]

$$\Delta q = -\frac{Z^2}{A}\frac{r_pN}{4\pi\beta^2\gamma^3\varepsilon}k_{\text{bunch}}. \tag{2.8}$$

For coasting beams, it is enough to put $k_{\text{bunch}} = 1$ in (2.7) and (2.8), which can be ascertained by repeating calculations (2.3)–(2.8) for $\rho(x,y,s)$ (1.2) at $x \ll \sigma_x$, $y \ll \sigma_y$.

*Beam–Beam Effect.* When particle 1 crosses counter-propagating particles of bunch 2, it gets a momentum increment under the effect of the electromagnetic field of the bunch,

$$\mathbf{\Delta p}_{12} = \int_{-\infty}^{\infty} \mathbf{F}_{12}(t)\,dt,$$

where (see (2.3))

$$\mathbf{F}_{12} = Z_1e\left(\mathbf{E}_2 + \frac{1}{c^2}[\mathbf{v}_1[\mathbf{v}_2,\mathbf{E}_2]]\right) = Z_1e\left(\mathbf{E}_2 - (\boldsymbol{\beta}_1,\boldsymbol{\beta}_2)\,\mathbf{E}_{\perp 2}\right).$$

Here $\boldsymbol{\beta}_{1,2} = \mathbf{v}_{1,2}/c$; $\mathbf{E}_2$ is the vector of the electric field of bunch 2 in the laboratory system at the location of particle 1; and $\mathbf{E}_{\perp 2}$ is its component transverse to the $s$ axis.

*This formula is valid for electrons (positrons) at $A = 1$ with replacement of $r_p$ with $r_e$, the classical electron radius.

The time dependence of the transverse coordinates of particle 1 in the laboratory system $x_{\alpha 1}(t)$ is found using the invariant $(x_{\alpha 1}(t))^2/B_{\alpha 1}(s(t))$ (Fig. 1 and formula (1.6)):

$$x_{\alpha 1}(s(t)) = x_{\alpha 1}(0)\sqrt{1+\left(\frac{s(t)}{B^*_{\alpha 1}}\right)^2}. \tag{2.9}$$

The longitudinal coordinate $s(t)$ is defined in (1.7), and $B^*_{\alpha 1} = B_{\alpha 1}(0)$ (1.6). The coordinates of particle 1 with respect to the center of bunch 2 is found using Fig. 1 and equalities (1.7) and (1.9):

$$x_{\alpha 2}(t) = x_{\alpha 1}(t), \quad \eta_2(\eta, s_0) = \eta + V s_0. \tag{2.10}$$

The particle momentum increment in the $(x,\ s)$ plane is defined by the $x$-component of the force $\mathbf{F}_{12}$

$$F_{x12} = Z_1 e\,(1 - (\boldsymbol{\beta}_1, \boldsymbol{\beta}_2))\, E_{x2}(t). \tag{2.11}$$

The component $E_{x2}$ of the bunch 2 field at the point $(x_1, 0, s(t))$ is found from (2.2):

$$E_{x2}(t) = \frac{2Z_2 e N_2}{\sigma_{x2}(t)\,(\sigma_{x2}(t)+\sigma_{y2}(t))\sqrt{2\pi}\sigma_{s2}} \exp\left(\frac{-\eta_2^2(t)}{2\sigma_{s2}^2}\right) x_1(t). \tag{2.12}$$

The transverse "$\sigma$ sizes" of bunch 2 on the coordinate $s(t)$, $\sigma_{x2}(t)$ and $\sigma_{y2}(t)$, are defined in (1.5) and (1.6) for the beta functions $B_{\alpha 2}(s)$ of the bunch 2 particles at the point $(x_1(t), 0, s(t))$, and $x_1(t)$ is the coordinate of particle 1 (2.9) at the same point. Note that particles 2 and 1 are at the point $s(t)$ at the time

$$t\,(s, \eta) = \frac{s - \eta}{v_1}.$$

This equality allows time dependence of the parameters to be transformed to their $s$ dependence.

In one collision, particle 1 receives a transverse momentum (average over many revolutions (!))

$$\Delta p_{x12}(\eta) = \int_{-t_1}^{t_2} F_{x12}\,(s(t))\, dt = \frac{4Z_1 Z_2 e^2 N_2}{\sigma_{s2}} \frac{1-(\boldsymbol{\beta}_1, \boldsymbol{\beta}_2)}{\beta_1 c} \Phi(\eta),$$

$$\Phi(\eta) = \frac{1}{\sqrt{2\pi}} \int_{-l_D}^{l_D} \frac{x_1(s)}{\sigma_{x2}(s)(\sigma_{x2}(s)+\sigma_{y2}(s))} \exp\left[-\frac{1}{2}\left(\frac{\eta_2(\eta, s)}{\sigma_{s2}}\right)^2\right] ds. \tag{2.13}$$

The coordinate $x_1(s)$ is defined in (2.9); and the parameters $\sigma_{\alpha 2}(s)$, in (1.5) and (1.6).



Multiple intersection of bunch 2 by particle 1 results in a betatron oscillation frequency shift $\xi_{12}$ (conventional designation). This is known as a parameter of the beam–beam effect (BB), or, briefly, the beam–beam tune shift.

The quantity $\xi_{12}$ can be found in the thin lens approximation by calculating the transition matrix for a particle revolution in the collider ring with allowance for perturbation of the particle motion by the electromagnetic field of counter bunch 2 (see Appendix). Knowing the transverse increment of the transverse component of particle 1 momentum $\Delta p_{x12}$ (2.13) and ignoring the change in the $x_1$ coordinate after one passage through bunch 2, one can replace bunch 2 by a thin lens with the focal length $f_{\mathrm{BB}}$

$$\frac{1}{f_{\mathrm{BB}}} = \frac{1}{x_1(0)} \frac{\Delta p_{x12}}{p_1}, \quad x_1(0) = \sqrt{\varepsilon_{x1} B^*_{x1}}. \tag{2.14}$$

Here $B^*_{x1}$ is the betatron function at the IP in the absence of the perturbing thin lens. The phase shift of betatron oscillations after each intersection is (formula (A.3) in Appendix)

$$\Delta\varphi = \frac{B^*_{x1}}{2 f_{\mathrm{BB}}}. \tag{2.15}$$

To this phase shift of betatron oscillations there corresponds their frequency tune shift

$$\xi_{x12} = \frac{\Delta\varphi}{2\pi} = \frac{B^*_{x1}}{4\pi} \frac{1}{x_1(0)} \frac{\Delta p_{x12}}{p_1}.$$

Substituting $f_{\mathrm{BB}}$ (2.14) and $\Delta p_{x12}$ (2.13), we obtain

$$\xi_{x12}(\eta) = \frac{Z_1 Z_2}{A_1} \frac{r_p N_2}{2\pi\varepsilon_{x2}} \frac{1-(\boldsymbol{\beta}_1, \boldsymbol{\beta}_2)}{\beta_1^2 \gamma_1} \frac{B^*_{x1}}{B^*_{x2}} \Phi_{x12}(\eta), \tag{2.16}$$

$$\Phi_{x12}(\eta) = \frac{1}{\sqrt{2\pi}} \int_{-l_D}^{l_D} \frac{\sqrt{1+\left(\frac{s}{B^*_{x1}}\right)^2}}{\sqrt{1+\left(\frac{s}{B^*_{x2}}\right)^2}\left(\sqrt{1+\left(\frac{s}{B^*_{x2}}\right)^2} + \sqrt{\frac{\varepsilon_{y2} B^*_{y2}}{\varepsilon_{x2} B^*_{x2}}}\sqrt{1+\left(\frac{s}{B^*_{y2}}\right)^2}\right)} \times \exp\left\{-\frac{1}{2}\left(\frac{\eta_2(\eta, s)}{\sigma_{s2}}\right)^2\right\} \frac{ds}{\sigma_{s2}}.$$

We underline that formula (2.16) describes the absolute value of the BB parameter. The choice of its sign is discussed at the beginning of Sec. 2.2.

The parameter $\Phi_{x12}(\eta)$, unlike $\Phi(\eta)$ (2.13), is here transformed to a dimensionless form. In addition, it is written in terms of emittances and beta functions of beams, which is convenient for numerical calculations. This parameter is an analogue of the known hourglass parameter (1.19) in luminosity formulas. The beam–beam effect parameters for the $y$-degree of freedom $\xi_{y12}$ and $\Phi_{y12}$ are obtained from (2.16) using the replacement $x \leftrightarrow y$. To estimate the beam–beam effect, it is sufficient to consider the case of $\eta \ll \sigma_s$. In this case, the parameter $\Phi_{x12}$ does not depend on $\eta$ and becomes constant. Here, as in the luminosity formulas in Sec. 1, one should set $l_D = 3B^*$ (1.31) for coaxial beams and (1.33) and (1.34) for intersecting beams.

Note that formula (2.16) differs from those encountered in the literature: they lack the parameter $\Phi_{x12}$ (at least, the author failed to find formulas that involve it) (see, for example, [21]).

In the case of identical counter-propagating axially symmetric beams with particles of equal velocities and with equal emittances in the axially symmetric focusing system of the collider

$$Z_1 = Z_2 = Z, \quad A_1 = A_2 = A, \quad v_1 = -v_2, \quad \boldsymbol{\beta}_1 = -\boldsymbol{\beta}_2 \equiv \boldsymbol{\beta}, \quad V = 2, \tag{2.17}$$

$$\varepsilon_{x1} = \varepsilon_{x2} = \varepsilon_{y1} \equiv \varepsilon, \quad \sigma_{s1} = \sigma_{s2} \equiv \sigma_s, \quad B^*_{x1} = B^*_{y1} = B^*_{x2} = B^*_{y2} \equiv B^*,$$

expressions (2.15) and (2.16) are greatly simplified: the parameters $\xi$ for both beams coincide and are

$$\xi_x(\eta) = \xi_y(\eta) = \frac{Z^2}{A}\frac{r_p N_2}{4\pi\varepsilon}\frac{1+\beta^2}{\beta^2\gamma}\lambda_0\Phi_x(\eta),$$

$$\Phi_{x,y12}(\eta = 0) = \frac{1}{\alpha}\frac{1}{\sqrt{2\pi}}\int\limits_{-l_D/B^*}^{l_D/B^*}\frac{1}{\sqrt{1+\chi^2}}\,\mathrm{e}^{-2(\chi/\alpha)^2}\,d\chi =$$

$$= \frac{1}{\sqrt{2\pi}}\int\limits_{-l_D/\sigma_s}^{l_D/\sigma_s}\frac{1}{\sqrt{1+(\alpha u)^2}}\,\mathrm{e}^{-2u^2}\,du, \tag{2.18}$$

$$\alpha = \frac{\sigma_s}{B^*}, \quad \chi = \frac{s_0}{B^*}, \quad u = \frac{s_0}{\sigma_s}.$$

When $\sigma_s \to 0$, we have $\alpha \to 0$ and accordingly obtain

$$\Phi_{x,y12}(\eta = 0) \to \frac{1}{\sqrt{2\pi}}\int\limits_{-\infty}^{\infty}\mathrm{e}^{-2u^2}\,du = 1.$$

As the emittance increases, the function $\Phi_{x,y12}$ monotonically decreases, being 0.913 at $\alpha = 1$ and 0.554 at $\alpha = 5$.



The beam–beam effect in the collision of a particle with a coasting beam is described by expressions (2.16) and (2.18), in which the bunch length $\sigma_s$ is taken to be equal to the ring circumference $C_{\text{ring}}$ (see Sec. 3.2).

Note that the betatron tune shifts $\Delta q$ and $\xi$ depend on the particle energy through the Lorentz factors $\beta$ and $\gamma$.

**2.2. Optimization of the Collider Luminosity.** In ion colliders the betatron tune shifts, both $\Delta q$ and $\xi$, have a negative value. This fact has a simple explanation: particles of both counter-propagating bunches have a positive charge (except for an exotic case of negatively charged ions of one of the beams). Therefore, the forces of the space charge of both the reference and the counter-propagating bunches are directed outward of the axis. This determines the signs of the betatron tune shifts (see formulas (2.5), (2.6)). The effect is different in electron–ion, electron–positron, and proton–antiproton colliders: the force of the counter-propagating beam is attractive, and the $\xi$-parameter is positive. Nevertheless, both effects influence independently on particle dynamics, and the process of beam instability development when the particle betatron frequency approaches the resonance value is rather complicated. Therefore, for simple estimates, the criterion of betatron oscillation stability can be the requirement that the sum of the moduli of the tune shifts does not exceed a certain maximum value:

$$|\Delta q| + |\xi| \leqslant \Delta Q_{\max}.$$

Further we use, for brevity, the symbols $\Delta q \equiv |\Delta q|$ and $\xi \equiv |\xi|$.

It is known from practice that an intense beam is stable (with all other conditions fulfilled) if

$$\Delta Q \leqslant 0.05. \tag{2.19}$$

It is the first optimization criterion. When choosing optimal parameters of collider beams, it is enough to ensure fulfillment of this condition for the largest of two pairs of parameters $\Delta q_x$, $\xi_x$ and $\Delta q_y$, $\xi_y$. We will consider the $x$-parameters as having the largest values (when $\sigma_x \ll \sigma_y$) and will thus concern ourselves with the problem of optimizing these very parameters.

Let us write the parameters of the first beam $\Delta q_1$ (2.7) and $\xi_{12}$ (2.15), (2.16) as

$$\Delta q_{x1} = \frac{Z_1^2}{A_1}N_1 a_{x1}, \quad \xi_{x12} = \frac{Z_1 Z_2}{A_1}N_2 b_{x1},$$

$$a_{x1} = \frac{r_p}{\pi\beta_1^2\gamma_1^3}\frac{\sqrt{\langle B_{x1}\rangle}\,k_{\text{bunch}1}}{\sqrt{\varepsilon_{x1}}\left(\sqrt{\varepsilon_{x1}\langle B_{x1}\rangle} + \sqrt{\varepsilon_{y1}\langle B_{y1}\rangle}\right)}, \tag{2.20}$$

$$b_{x1} = \frac{r_p}{2\pi\varepsilon_{x2}}\frac{1-(\boldsymbol{\beta}_1,\boldsymbol{\beta}_2)}{\beta_1^2\gamma_1}\frac{B^*_{x1}}{B^*_{x2}}\Phi_{x12}(\eta)$$

and do the same for the parameters of the second beam $\Delta q_2$ and $\xi_{21}$, making the replacement $1 \leftrightarrow 2$. Then we write two equations:

$$\begin{aligned} \Delta q_{x1} + \xi_{x12} &= \Delta Q_{x1}, \\ \Delta q_{x2} + \xi_{x21} &= \Delta Q_{x2}. \end{aligned} \tag{2.21}$$

Now it would seem possible, on demanding that condition (2.19) be fulfilled for both beams ($\Delta Q_{1,2} \leqslant 0.05$) and writing the parameters $\Delta q$ and $\xi$ in the form (2.20), to obtain a system of two algebraic equations in $N_1$ and $N_2$:

$$\begin{aligned} \frac{Z_1^2}{A_1} a_{x1} N_1 + \frac{Z_1 Z_2}{A_1} b_{x1} N_2 &= \Delta Q_{x1}, \\ \frac{Z_2^2}{A_2} a_{x2} N_2 + \frac{Z_1 Z_2}{A_2} b_{x2} N_1 &= \Delta Q_{x2}. \end{aligned} \tag{2.22}$$

Note that these equations are interrelated through the BB effect in terms of the parameters $\xi_{x12}$ and $\xi_{x21}$. However, an attempt to straightforwardly solve this system of equations reveals that at particular energies the determinant of the system vanishes, which means that there is no solution. Therefore, the beam parameters have to be optimized on the basis of physical and obvious mathematical considerations.

Let us assume that both the collider rings and colliding beams 1 and 2 are tuned so that their Laslett shifts are equal (the second optimization condition):

$$\Delta q_{x1} = \Delta q_{x2} \equiv \Delta q_x. \tag{2.23}$$

Then the number of particles in the bunches of these beams satisfies the condition (see (2.20))

$$\frac{N_1}{N_2} = \frac{A_1}{Z_1^2} \frac{Z_2^2}{A_2} \frac{a_{x2}}{a_{x1}}. \tag{2.24}$$

Substituting $N_1/N_2$ (2.24) into the ratio of the parameters $\Delta q/\xi$, we obtain

$$\frac{\Delta q_x}{\xi_{x12}} = \lambda_0 \frac{a_{x2}}{b_{x1}}, \quad \frac{\Delta q_x}{\xi_{x21}} = \frac{1}{\lambda_0} \frac{a_{x1}}{b_{x2}}. \tag{2.25}$$

These relations allow the parameters $\xi_{x12}$ and $\xi_{x21}$ to be eliminated from equations (2.21), and system of equations (2.22) involves only three unknowns — $\Delta q_x$, $\Delta Q_{x1}$, and $\Delta Q_{x2}$:

$$\begin{aligned} \Delta q_x \left(1 + \frac{b_{x1}}{\lambda_0 a_{x2}}\right) &= \Delta Q_{x1}, \\ \Delta q_x \left(1 + \frac{\lambda_0 b_{x2}}{a_{x1}}\right) &= \Delta Q_{x2}. \end{aligned} \tag{2.26}$$



It follows that the shifts $\Delta Q_{x1}$ and $\Delta Q_{x2}$ are not independent parameters. Choosing, for example, the value $\Delta Q_{x1}$, we unambiguously determine the values $\Delta q_x$ and $\Delta Q_{x2}$:

$$\Delta q_x = \frac{\lambda_0 a_{x2}}{\lambda_0 a_{x2} + b_{x1}} \Delta Q_{x1}, \quad \Delta Q_{x2} = \frac{a_{x1} + \lambda_0 b_{x2}}{\lambda_0 a_{x2} + b_{x1}} \frac{\lambda_0 a_{x2}}{a_{x1}} \Delta Q_{x1}. \tag{2.27}$$

Then we find $\xi_{x12}$ and $\xi_{x21}$ from (2.25) and $N_1$ and $N_2$ from (2.20). Thus, all parameters needed for luminosity calculations are determined.

Generally speaking, the first criterion can be violated so that the function $\Delta Q_{x2}(E_{\text{ion}})$ grows above the limiting value (e.g., 0.05). In this case, $\Delta Q_{x1}$ has to be decreased until $\Delta Q_{x2}$ drops below 0.05.

The presented method for optimization of collider parameters imposes limits on the intensity of the colliding beams and thus on the collider luminosity. But this does not mean that there is no way to increase luminosity. Indeed, the above optimization was performed for the chosen values of the focusing system parameters ($B^*$), beam emittances ($\varepsilon$), and longitudinal bunch sizes ($\sigma_s$) for bunched beams. Actually, three sets of these parameters remain free. Their choice determines the luminosity after the optimization. And they have their own limits.

Let us begin with the emittance. As follows from general formula for luminosity (1.15) and its particular cases, luminosity is proportional to a product of the numbers of particles in the colliding beams (or their bunches) $N_1$ and $N_2$ and inversely proportional to the beam emittances. The maximum number of particles is in turn directly proportional to the emittance, as follows from (2.20). As a result, luminosity is also directly proportional to the emittance:

$$L \propto \frac{N_1 N_2}{\varepsilon} \propto \varepsilon. \tag{2.28}$$

Thus, luminosity can be increased by increasing emittances of colliding beams and accordingly the number of particles in them (!). But sooner or later the intensity in the injection system of the collider complex comes to its limit.

Influence of two other parameters is less obvious. Luminosity (1.15) is inversely proportional to the beta function at the interaction point $B^*$ and depends on the relation $\alpha = \sigma_s/B^*$, the so-called hourglass effect. This effect is particularly manifested for two identical bunched beams (1.19). The function $\Phi_{\text{HG}}(\alpha)$ monotonically decreases from 1 at $\alpha = 0$ to 0.287 at $\alpha = 5$, and it thus follows that longitudinal compression of the bunch at the constant number of particles in the beams (bunches) does not give a considerable increase in the luminosity at $\sigma_s < B^*$. For example, $\Phi_{\text{HG}}(1) = 0.7578$.

At the same time, the maximum number of particles in bunched beams is proportional to the bunch length ($1/k_{\text{bunch}}$). Consequently, dependence of luminosity on the longitudinal bunch size is similar to its dependence on the emittance: increasing the bunch length, one can increase luminosity proportionally to the bunch length $\sigma_s$, simultaneously increasing the number of particles in a bunch. However, in addition to "technical" limits of intensity, there arises a bunch length limit due to the requirement of localization of the beam collision region (see Sec. 1.5 and Fig. 2). In fact, one has to choose between the amount of luminosity and the acceptance of the detector.

Examples of the application of the presented method for optimization of collider parameters are given in Sec. 3.

## 3. EXAMPLES OF OPTIMIZATION OF THE CYCLIC COLLIDER LUMINOSITY

In this section we give four examples of choosing optimal parameters for different versions of cyclic ion colliders, including the electron–ion and merging-beam colliders. The parameters of the collider and its beams are formulated in each example.

**3.1. NICA Ion Collider in the Symmetric Mode.** The symmetric mode of the ion phase of the NICA collider implies collision of two bunches of $^{197}Au^{79+}$ nuclei at one IP (Table 1).

In this section the parameter $\lambda$ is unity due to the symmetry of both the beams and the focusing system.

As the calculations show (Fig. 4, *a*), the effect that governs the beam intensity and consequently the luminosity is the Laslett effect ($\Delta q$ (2.7), (2.8)). The BB effect ($\xi$ (2.16), (2.18)) becomes noticeable at an energy above 3 GeV/u. The sum of the betatron frequency shifts $\Delta q$ and $\xi$ remains constant, $\Delta Q_1 = \Delta Q_2 = 0.05$. The parameter $\Phi_{12}$ (2.16) is 0.457.

The maximum luminosity calculated by formula (1.19) (Fig. 4, *b*) amounts to $5.7 \cdot 10^{27}$ cm$^{-2} \cdot$ s$^{-1}$ at the energy of 4.5 GeV/nucleon. But this requires a rather high beam intensity with $6.9 \cdot 10^9$ ions per bunch.

**Table 1. Parameters of the NICA collider at the collision of gold nuclei (symmetric mode)**

| Parameter | Rings 1 and 2 |
|---|---|
| Ring circumference, m | 503.04 |
| Ions | $^{197}Au^{79+}$ |
| Ion energy, GeV/nucleon | 1.0–4.5 |
| Minimum beta function at IP $B^*$, cm | 60 |
| Ion bunch emittance, $\pi \cdot$ mm $\cdot$ mrad | 1.1 |
| Bunch length $\sigma_s$, cm | 60 |
| Betatron tune $Q_x$ | 9.44 |



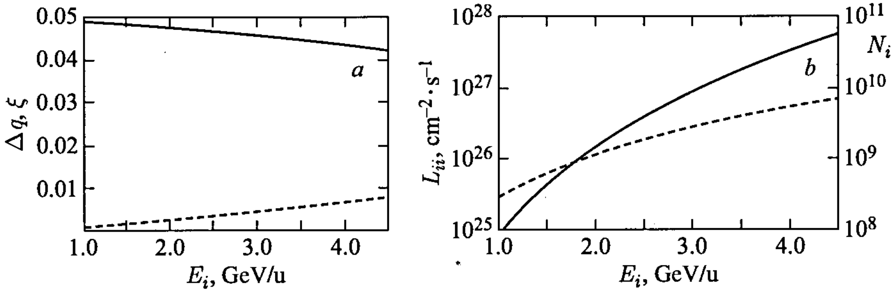


Fig. 4. Dependence of the parameters of the ion collider with the bunched $^{197}Au^{79+}$ beams on the ion energy $E_i$; $\Delta Q = 0.05$: *a*) Laslett parameter $\Delta q$ (solid curve) and the BB parameter $\xi$ (dashed curve); *b*) collider luminosity $L_{ii}$ (solid curve) and the number of particles per bunch $N_i$ (dashed curve)

As the energy of colliding particles increases, the space charge effects reverse the roles: the parameter of the space charge effect is larger than the Laslett parameter. This is demonstrated in collisions of proton beams, which are planned in the NICA project [1], with polarized protons and deuterons (Fig. 5).

The symmetric mode of two identical coasting beams (Fig. 6) convincingly shows how their being unbunched affects the luminosity: it (formula (1.29)) decreases by a few orders of magnitude. This is an almost obvious result. Less obvious is that the main limitation is the BB effect (Fig. 6, *a*).

The luminosity is calculated by formulas (1.28) and (1.29). Here the emittance of the coasting beams was increased to 11 $\pi \cdot$ mm $\cdot$ mrad, which, in accordance with (2.28), led to a proportional 10-fold increase in the luminosity.

As compared to the previous case of bunched $^{197}Au^{79+}$ ion beams (Fig. 4), the parameters of the BB effect and the Laslett effect changed places, and now the beam intensity limits the BB effect.

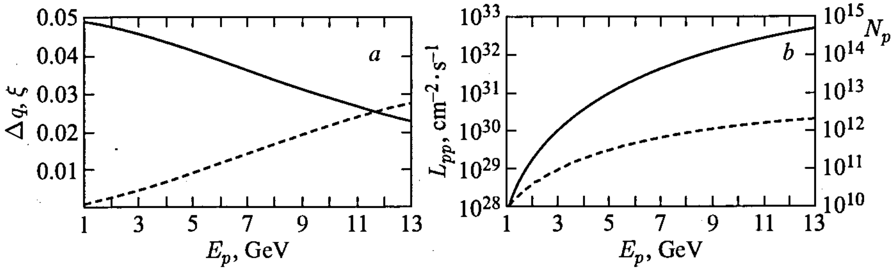


Fig. 5. Dependence of the parameters of the proton–proton collider on the proton energy $E_p$; $\Delta Q = 0.05$: *a*) Laslett parameter $\Delta q$ (solid curve) and the BB parameter $\xi$ (dashed curve); *b*) collider luminosity $L_{pp}$ (solid curve) and the number of particles per bunch $N_p$ (dashed curve)

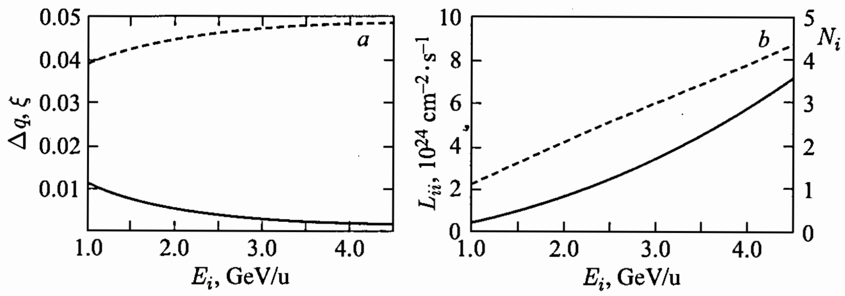


Fig. 6. Dependence of the parameters of the ion–ion collider with the coasting $^{197}Au^{79+}$ beams on the ion energy $E_i$; beam emittances are $11\,\pi\cdot$mm$\cdot$mrad. *a*) Laslett parameter $\Delta q$ (solid curve) and the BB parameter $\xi$ (dashed curve); *b*) collider luminosity $L_{ii}$ (solid curve) and the number of particles in a beam $N_i$ (dashed curve)

**3.2. NICA Collider in the Asymmetric Mode.** As an example of an asymmetric collider, we consider the NICA collider with colliding proton and deuteron beams. This problem appears in the nucleon spin physics studies, when it is possible to discriminate between proton–proton and proton–neutron collisions. Of interest are both the cases of the resting center of mass (c.m.) of two colliding nucleons (*pp* or *pn*) and the case of the c.m. of the proton–deuteron system. In the first case, the proton and deuteron velocities are equal, and in the second case the deuteron velocity is lower than the proton velocity:

$$\beta_N = \frac{\beta_p}{\sqrt{A_\mu^2 + \beta_p^2\left(1 - A_\mu^2\right)}}. \tag{3.1}$$

Here $\beta_N$ and $\beta_p$ are the velocities of the nucleus (deuteron) and the proton in units of the speed of light, $A_\mu = \mu A_N$, $\mu$ is the ratio of the nuclear nucleon mass to the proton mass, and $A_N$ is the atomic weight of the nucleus. This mode is of interest for studying possible tensor polarization in *pd* collisions. To calculate these collision modes, one should insert

$$V = 1 + \frac{\beta_p}{\beta_N}$$

into the corresponding luminosity formulas and write $1+\beta_N\beta_p$ instead of $1+\beta^2$ in (2.16) and (2.18). In addition, in this proton–nucleus collision mode, when one of the beams is coasting, synchronization is optimal due to the difference in the proton and deuteron velocities.

The results of the calculations for proton–nucleon collisions (i.e., in the proton and nuclear nucleon center-of-mass systems) at the NICA collider with the bunched deuteron and proton beams are given below (Fig. 7). Luminosity in proton–nucleon collisions is calculated by formula (1.19). The beams have equal emittances of $1.1\ \pi\cdot$mm$\cdot$mrad. The particle energy in the collider is



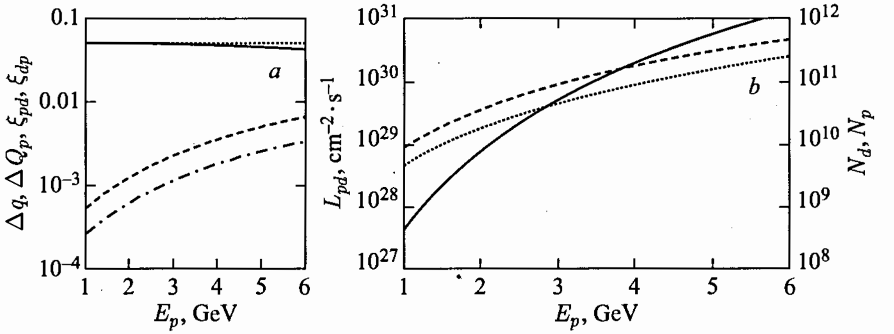


Fig. 7. Dependence of the parameters of the ion collider with the bunched deuteron and proton beams on the proton energy $E_p$; beam emittances are $1.1\ \pi\cdot$mm$\cdot$mrad, $B^* = 3$ m: *a*) Laslett parameter $\Delta q$ (solid curve), the total betatron tune shift for protons $\Delta Q_p$ (dotted curve), and the BB parameter for protons on a deuteron bunch $\xi_{pd}$ (dashed curve) and deuterons on a proton bunch $\xi_{dp}$ (dash-dotted curve); *b*) collider luminosity $L_{pd}$ (solid curve) and the number of particles in a deuteron bunch $N_d$ (dashed curve) and a proton bunch $N_p$ (dotted curve)

1–6 GeV/nucleon, and $\sqrt{s_{NN}}$ = 3.87–13.87 GeV. The other parameters are the same as in Table 1. The parameter $\lambda$ is put equal to unity because the NICA collider is supposed to have a unique beam convergence system, where convergence magnets are placed closer to the IP than the final focus lenses, which allows their independent tuning. In this example, the main limitation for the beam intensities and thus for the luminosity is also the Laslett effect.

**3.3. Electron–Ion Collider with an Equilibrium Ion Beam.** The electron–ion collider with coasting and bunched beams can become an important nuclear-physics tool for studying rare and radioactive isotopes. This collider is likely to feature a very low ion beam intensity. It was proposed to solve its luminosity problem by using the so-called crystalline, or ordered, ion beam.

The idea of this beam was proposed by V. V. Parkhomchuk in 1985 after successful experiments on suppression of the proton beam noise and compression of the proton beam in the NAP–M electron-cooled storage ring at the Institute of Nuclear Physics (Novosibirsk). In the 1990s, the experiments were repeated at several laboratories around the world, and the beam compression process was thoroughly investigated. Soon the first proposals of colliders with crystalline beams were put forward [22, 23]. However, further analysis showed that the intensity of the crystalline beams was quite low, and the luminosity of this collider would consequently be very low (see [9] for details). In a few independent experiments it was found that the crystalline (ordered) beam, which was a chain of ions circulating in a storage ring, has a linear density

$$\left(\frac{dN_{\text{ion}}}{ds}\right) \leqslant 3\cdot 10^5\ \text{ions/m}. \tag{3.2}$$

The main advantages of the ordered beams are their very low emittance and particle momentum spread

$$\varepsilon \sim 0.1\text{–}1.8\ \text{nm}, \quad \Delta p/p \underset{\sim}{<} (1\text{–}5)\cdot 10^{-6}\ (1\sigma).$$

Transition of the beam to the ordered state occurs abruptly as the beam density drops down to the critical value of about 90 ions/m. The transverse size of the beam and the momentum spread decrease by almost an order of magnitude. This is a sort of phase transition from the quasi-ordered state to the ordered one (Fig. 8).

For bunched ordered beams, condition (3.2) is also fulfilled, but it is now the linear bunch density and not the average beam density. Therefore, it makes sense to use the bunched beam when there is a considerable deficit of ions.

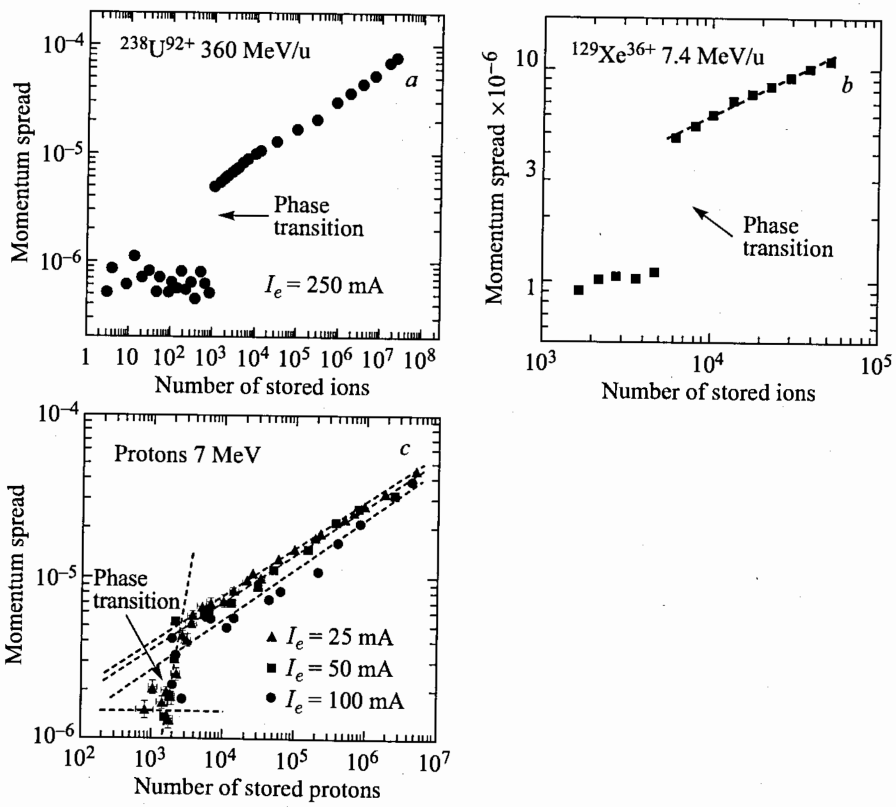


Fig. 8. Dependence of the momentum spread ($1\sigma$) on the number of beam particles in the electron-cooled storage rings: *a*) $^{238}U^{92+}$ in the ESR [24], *b*) $^{129}Xe^{36+}$ in CRYRING [25], *c*) protons in the S-LSR [26]



Of practical interest is another property of these deep cooled ion beams: in the supercritical state the transverse size and the momentum spread increase from value (3.2) with increasing linear density in compliance with the law

$$\sigma_\perp(N_i) = \sigma_{\text{transition}} \left(\frac{N}{N_{\text{transition}}}\right)^{1/3}. \tag{3.3}$$

This law is valid up to the maximal linear density of about $5\cdot 10^5$ ions/m [9]. And it is the result of the equilibrium between the external cooling of ions by the electron beam and the internal heating by the so-called intrabeam scattering — Coulomb scattering of beam ions off one another. Law (3.3) was experimentally verified for coasting beams.

It is planned to use the equilibrium ion beam (3.3) in the electron–ion collider of the DERICA project (Dubna Electron–Radioactive Isotope Collider fAcility) [27]. Table 2 presents possible parameters of the collider and its luminosity at collisions of electron bunches with the equilibrium ion beam (see [9] for details). It is assumed that the scheme of intersecting beams is used in the collider (Sec. 1.6). Therefore, $\lambda = 1$. The angle $\phi$ (1.32) is taken to be negligibly small. The luminosity is calculated by formula (1.25).

The estimates (Fig. 9) show that the equilibrium beam has a slightly higher luminosity than the bunched beam with a constant emittance until their trans-

**Table 2. Parameters of the electron–ion collider**

| Particles of collider beams | $^{238}U^{92+}$ ions | Electrons |
|---|---|---|
| Beam | Equilibrium coasting | Bunched |
| Ring circumference, m | 18.56* | 16.0 |
| Particle energy, MeV/u, MeV | 300 | 500 |
| Revolution frequency, MHz | 10.547 | 18.75 |
| Number of particles in beam, bunch | $1\cdot 10^3$–$1\cdot 10^7$ | $10^{10}$ |
| Number of bunches | — | 9 |
| Bunch length, cm | — | 4 |
| Beam emittance, nm | 0.01–170 | 50 |
| Transverse bunch size, $\mu$m | $\leqslant 220$ | 220 |
| Laslett tune shift $\Delta q$ | $\leqslant 0.004$ | $7.6\cdot 10^{-5}$ |
| BB tune shift $\xi_{ie}$, $\xi_{ei}$ | 0.08 | $\leqslant 0.01$ |
| Beta function $B^*$ at IP, m | 1.0 | 1.0 |
| Luminosity, $\text{cm}^{-2}\cdot\text{s}^{-1}$ | $7.5\cdot 10^{23}$–$1.7\cdot 10^{27}$ | |

*The ring circumference is chosen so that synchronization condition (1.35) necessary for the bunched ion beam is fulfilled.

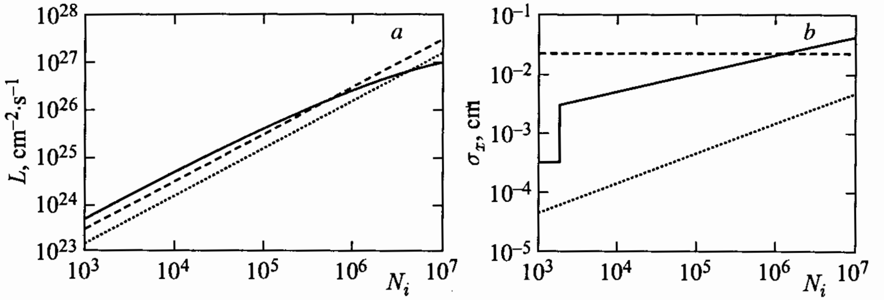


Fig. 9. Dependence of the luminosity ($a$) and the transverse beam size $\sigma_x$ ($b$) on the number of ion beam particles: the cooled coasting ion beam below and above the phase transition (solid curves), the bunched ion beam with a constant emittance equal to the electron beam emittance (50 nm) (dashed curves), and the bunched ion beam with an emittance limited by the space charge (Laslett parameter) (dotted curves)

verse sizes become equal and is "outplayed" by the latter when the size of the equilibrium ion beam exceeds the transverse size of the electron beam.

There are different causes why the ion and electron beam intensities are limited in this collider. The maximum number of particles in the ion beam is determined by the condition of maintaining the small transverse size of the bunch (3.3). The electron bunch intensity is dictated by the BB effect produced by this bunch on ions. In the numerical example, the parameter $\xi_{ie}$ has the value that can be achieved only at the effective electron cooling of the ion beam. This, by the way, is also necessary for formation of an equilibrium ion beam.

The necessity to use a coasting ion beam is caused by the collision synchronization requirements, which are fundamental in this case. Velocities of relativistic electrons and ions are considerably different, as is demanded by the experiment itself set up at this kind of collider [17]. Therefore, condition (1.35) can be satisfied for the bunched electron and ion beams only at strictly determined (discrete) particle parameters and ring sizes. But this rules out a possibility of smooth particle energy scanning, which is usually needed in nuclear-physics investigations. The problem is eliminated in ultrarelativistic electron–ion colliders, where velocities of electrons and heavy particles almost do not differ from the speed of light. These colliders are under development at CERN (LHeC) and two US laboratories, BNL (eRHIC) and JLab (MEIC).

Low intensity of equilibrium beams limits the area of their application to physics of rare (exotic) and radioactive isotopes [27].

**3.4. Merging Ion Beams.** The first proposal to use storage rings with electron cooling in nuclear-physics experiments [28] appeared in the late 1970s as the electron cooling method was under development at the Institute of Nuclear Physics (Novosibirsk). These experiments were started almost ten years later, when electron-cooled storage rings were built in several nuclear-physics laboratories.



**Table 3. Parameters of the collider with merging beams**

| Beam particles | $^{238}U^{92+}$ | $^{235}U^{92+}$ |
|---|---|---|
| Beam | Coasting | Coasting |
| Ring circumference, m | 76.22 | 62.86 |
| Particle energy, MeV/u | 785 | 500 |
| Magnetic field of dipoles, T | 1.5 | 1.5 |
| Number of particles in a beam | $4.9 \cdot 10^{10}$ | $2.35 \cdot 10^{10}$ |
| Beam emittance, $\pi \cdot$ mm $\cdot$ mrad | 1.1 | 1.1 |
| Laslett tune shift $\Delta q$ | 0.043 | 0.043 |
| BB tune shift $\xi_{12}$, $\xi_{21}$ | 0.007 | 0.002 |
| Beta function $B^*$ at IP, m | 2.0 | 2.0 |
| Interaction region length, m | 6.0 | |
| Luminosity, cm$^{-2} \cdot$ s$^{-1}$ | $2.4 \cdot 10^{25}$ | |

The most extensive investigations were carried out at the Experimental Storage Ring (ESR) at the GSI (Darmstadt, Germany). At that time, it was proposed [29] to set up experiments at a collider with merging beams, whose particles move in the interaction region in the same direction at different velocities (energies). An experiment set up in this way opens up new possibilities for structure studies of radioactive nuclei.

One of the possible applications of a merging-beam collider proposed in [30] is the study of vacuum physics in collisions of heavy nuclei, which give rise to a "supercritical" electric field that separates particles of a virtual electron–positron pair. This problem has been discussed for a long time. In a particular experimental scheme (Table 3), colliding particles are nuclei of two uranium isotopes $^{238}U^{92+}$ and $^{235}U^{92+}$ with their total center-of-mass energy chosen to be 6 MeV/u. This is enough to pass over the Coulomb barrier. It is also proposed to use the intersecting-beam scheme (Sec. 1.6) or the NICA collider scheme with colliding deuteron–proton beams (see above).

The collision synchronization problem is solved, as in the previous section, by using two coasting beams.

The collider luminosity is limited by the Laslett effect, which is due to relatively low energy of heavy nuclei. It is calculated by formulas (1.28) and (1.29), and, as assumed in [30], it is quite sufficient for the proposed experiment.

## CONCLUSIONS

The above collider luminosity formulas for three different collision modes — two bunched beams, two coasting beams, and a bunched and a coasting beam — describe all possible applications of cyclic colliders. The proposed method for optimization of the ion collider parameters allows their limiting values to be determined and thus the maximum possible collider luminosity to be found. The main criteria limiting the luminosity, which are suggested and used in the numerical examples, are two space charge effects of the colliding beams, the frequency shift of the transverse (betatron) particle oscillations under the action of the intrinsic electromagnetic field of the bunch (Laslett effect) and the frequency shift of the counter bunch field (BB effect). Collision synchronization conditions are formulated, which show the advantage of the coasting beam for the asymmetric collider (Sec. 3.2). The numerical examples demonstrate the cases where the Laslett effect is crucial (Secs. 3.1, 3.2 for bunched ion beams, Sec. 3.3 for an electron beam, and Sec. 3.4 for coasting ion beams) and the cases where luminosity is limited by the BB effect (Sec. 3.1, coasting ion beams, and Secs. 3.2, 3.3). In Sec. 3.1, an intermediate case with colliding proton beams is shown, where the BB effect prevails at high energies.

**Acknowledgements.** The author is grateful to V. A. Lebedev, S. S. Nagaitsev, and E. B. Levichev for helpful discussions, D. Jovett and S. Yamaguchi for providing valuable information, D. N. Shatilov and A. O. Sidorin for numerous critical comments and recommendations on the manuscript, Zh. L. Mal'tseva for valuable advice during numerical calculations, and S. A. Melnikov for careful check of the the calculations and proper corrections.

The work was performed in connection with the implementation of the NICA [1] and DERICA [27] projects at JINR. The author thanks his colleagues for working together on these projects.

## Appendix

## THIN LENS APPROXIMATION

The frequency shift of betatron oscillations $\xi_{12}$ due to the beam–beam effect can be found by multiplying the transition matrix for the particle revolution in the collider ring (so-called Twiss matrix)

$$M_{\rm ring} = \begin{pmatrix} \cos\varphi_0 + \alpha\sin\varphi_0 & \beta\sin\varphi_0 \\ -\gamma\sin\varphi_0 & \cos\varphi_0 - \alpha\sin\varphi_0 \end{pmatrix}, \quad \varphi_0 = 2\pi Q,$$

by the thin lens matrix

$$M_f = \begin{pmatrix} 1 & 0 \\ -\frac{1}{f} & 1 \end{pmatrix},$$

where the focal length $f$ of the thin lens must be related to the phase shift of the betatron oscillations.



Considering the perturbation introduced by the thin lens, we find the transition matrix $M^*$ by multiplying the matrices $M_{\rm ring}$ and $M_f$:

$$M^* = M_{\rm ring}M_f = \\ = \begin{pmatrix} \cos\varphi_0 + \alpha_0\sin\varphi_0 - \frac{\beta_0}{f}\sin\varphi_0 & \beta_0\sin\varphi_0 \\ -\gamma_0\sin\varphi_0 - \frac{1}{f}\cos\varphi_0 + \frac{\alpha_0}{f}\sin\varphi_0 & \cos\varphi_0 - \alpha_0\sin\varphi_0 \end{pmatrix}. \quad \text{(A.1)}$$

Representing the terms of the matrix $M^*$ as

$$\varphi^* = \varphi_0 + \Delta\varphi, \quad \Delta\varphi \ll \varphi_0; \quad \beta = \beta_0 + \Delta\beta; \quad \alpha = \alpha_0 + \Delta\alpha, \quad \gamma = \gamma_0 + \Delta\gamma,$$

where $\Delta\varphi$, $\Delta\alpha$, $\Delta\beta$, $\Delta\gamma$ are the perturbations introduced by the thin lens, we write the matrix $M^*$ as

$$M^* \equiv M_\Delta = \begin{pmatrix} \cos\varphi^* + \alpha\sin\varphi^* & \beta\sin\varphi^* \\ -\gamma\sin\varphi^* & \cos\varphi^* - \alpha\sin\varphi^* \end{pmatrix}. \quad \text{(A.2)}$$

Equating the corresponding terms of matrices (A.1) and (A.2), we obtain in the linear $\Delta$-term approximation

$$\begin{aligned} m_{11}^* &= m_{11}^\Delta \to -\frac{\beta_0}{f}\sin\varphi_0 = -\Delta\varphi\,(\sin\varphi_0 - \alpha_0\cos\varphi_0) + \Delta\alpha\sin\varphi_0, \\ m_{12}^* &= m_{12}^\Delta \to 0 = \beta_0\cos\varphi_0\Delta\varphi + \Delta\beta\sin\varphi_0, \\ m_{21}^* &= m_{21}^\Delta \to -\frac{\cos\varphi_0}{f} + \frac{\alpha_0\sin\varphi_0}{f} = \gamma_0\Delta\varphi\cos\varphi_0 - \Delta\gamma\sin\varphi_0, \\ m_{22}^* &= m_{22}^\Delta \to 0 = -\Delta\varphi\,(\sin\varphi_0 + \alpha_0\cos\varphi_0) - \Delta\alpha\sin\varphi_0. \end{aligned}$$

Thus, we obtained four equations in the unknowns $\Delta\varphi$, $\Delta\alpha$, $\Delta\beta$, and $\Delta\gamma$:

$$\begin{aligned} &\Delta\varphi\,(\sin\varphi_0 - \alpha_0\cos\varphi_0) - \Delta\alpha\sin\varphi_0 = \frac{\beta_0}{f}\sin\varphi_0, \\ &\Delta\varphi\beta_0\cos\varphi_0 + \Delta\beta\sin\varphi_0 = 0, \\ &-\Delta\varphi\gamma_0\cos\varphi_0 - \Delta\gamma\sin\varphi_0 = -\frac{1}{f}(\cos\varphi_0 - \alpha_0\sin\varphi_0), \\ &\Delta\varphi\,(\sin\varphi_0 + \alpha_0\cos\varphi_0) + \Delta\alpha\sin\varphi_0 = 0. \end{aligned}$$

Solving this system of linear equations by the known determinant calculation method, we find the determinant of the system $\mathrm{Det}_\Delta = -2\sin^4\varphi_0$ and the determinant with the replacement of the first column in $\mathrm{Det}_\Delta$ by the coefficients of the right-hand side of the system $\mathrm{Det}_\varphi = -(\beta_0/f)\sin^4\varphi_0$. Their ratio yields the desired phase shift $\varphi$ in the presence of the thin lens:

$$\Delta\varphi = \frac{\mathrm{Det}_\varphi}{\mathrm{Det}_\Delta} = \frac{\beta_0}{2f}. \tag{A.3}$$

This expression for $\Delta\varphi$ exactly coincides with (2.15), since $\beta_0 \equiv B^*_{x1}$ is the betatron function at the location of the "perturbing" thin lens (when it is not there), and the focal length is $f \equiv f_{\mathrm{BB}}$.

## REFERENCES


1. *Agapov N. N., Kekelidze V. D., Kovalenko A. D., Lednický R., Matveev V. A., Meshkov I. N., Nikitin V. A., Potrebenikov Yu. K., Sorin A. S., Trubnikov G. V.* Relativistic Nuclear Physics at JINR: From the Synchrophasotron to the NICA Collider // Phys. Usp. 2016. V. 59. P. 383–402.
2. *Carrigan R., Lebedev V., Mokhov N., Nagaitsev S., Stancari G., Still D., Valishev A.* Emittance Growth and Beam Loss // Accelerator Physics at the Tevatron Collider / Eds.: V. Lebedev, V. Shiltsev. New York: Springer, 2014. P. 254.
3. Handbook of Accelerator Physics and Engineering / Eds.: A. W. Chao, K. N. Mess, M. Tigner, F. Zimmermann. 2nd Ed. Singapore: World Sci. Publ., 2013. 311 p.
4. *Syphers M. J., Zimmermann F.* Luminosity. Accelerator Physics of Collider. http://pdg.lbl.gov/2015/reviews/rpp2015-rev-accel-phys-colliders.pdf. 2015. P. 14.
5. *Gareyte J.* Quality Limitations of Hadron Beams // High Quality Beams: Joint US–CERN–Japan–Russia Accel. School, St. Petersburg–Moscow, Russia, July 1–14, 2000. Melville; New York: AIP Conf. Proc., 2001. V. 592. P. 26.
6. *Batygin Y., Katayama T.* Luminosity of Particle Collider. RIKEN Commun. RIKEN-AT-AC-10. Wako, 1998. 21 p.
7. *Meshkov I. N.* Luminosity of a Collider with Asymmetric Beams // Phys. Part. Nucl. Lett. 2018. V. 15, No. 5. P. 506–509; http://arXiv.org/abs/1802. 08447v2.
8. *Meshkov I. N.* Optimum Luminosity of Proton–Ion Collider // Proc. of RuPAC'2018. jacow TUCBMNH01.
9. *Meshkov I. N.* Electron–Ion Collider with Quasi-Ordered Ion Beam // Nucl. Instr. Meth. A. 2019. V. 917. P. 56–60; http://arXiv.org/abs/1806.08983.
10. *Jowett J.* Private Commun.
11. *Jamaguchi S.* Private Commun.
12. *Palmer R. B.* Energy Scaling, Crab Crossing and the Pair Problem. SLAC-Pub-4707. Stanford, 1988. 7 p.
13. *Raimondi R., Shatilov D., Zobov M.* Beam–Beam Issues for Colliding Schemes with Large Piwinski Angle and Crabbed Waist. LNF-07/003-IR. 2007; arXiv:physics/0702033.





14. *Raimondi P., Shatilov D., Zobov M.* Beam–Beam Simulations for Particle Factories with Crabbed Waist // Proc. of Part. Accel. Conf. (PAC 07), Albuquerque, New Mexico, 2007. P. 1469.
15. *Raimondi P., Shatilov D., Zobov M.* Supression of Beam–Beam Resonances in Crab Waist Collisions // Proc. of the 11th Eur. Part. Accel. Conf. (EPAC 08), Magazzini del Cotone, Genoa, Italy, 2008. P. 2620.
16. *Zobov M.* New Generation Electron–Positron Factories // Part. Nucl. 2011. V. 42, No. 3. P. 1479–1511.
17. *Antonov A. N., Gaidarov M. K., Ivanov M. V., Kadrev D. N.* The Electron–Ion Scattering Experiment ELISe at the International Facility for Antiproton and Ion Research (FAIR) — A Conceptual Design Study // Nucl. Instr. Meth. A. 2011. V. 637. P. 60–76; *Koop I. A. (BINP – GSI Collab.).* Conceptual Design on an Electron–Nucleus Scattering Facility at GSI // Proc. of Eur. Part. Accel. Conf. (EPAC 02), Paris, 2002. P. 620.
18. *Meshkov I. N.* Transport of Charged-Particle Beams. Novosibirsk: Nauka, 1991 (in Russian).
19. *Machida S.* Tune Shift and Tune Spread // High Quality Beams: Joint US–CERN–Japan–Russia Accel. School, Moscow–St. Petersburg, 2001. V. 592. P. 408.
20. *Laslett L. J.* Proc. of 1963 Summer Study on Storage Rings. BNL-7534. Brookhaven, 1963. 324 p.
21. *Seeman J. T.* Beam–Beam Parameter and Tune Shift // High Quality Beams: Joint US–CERN–Japan–Russia Accel. School, Moscow–St. Petersburg, 2001. V. 592. P. 165.
22. *Meshkov I., Sidorin A., Smirnov A., Syresin E., Katayama T.* Ordered State of Ion Beams. Preprint RIKEN-AF-AC-34. Japan, 2002. 15 p.
23. *Meshkov I., Mohl D., Katayama T., Sidorin A., Smirnov A., Syresin E., Trubnikov G., Tsutsui H.* Numerical Simulation of Crystalline Beam in Storage Ring // Nucl. Instr. Meth. A. 2004. V. 532. P. 376–381.
24. *Steck M., Beckert K., Beller P., Franzke B., Nolden F.* Anomalous Temperature Reduction of Electron-Cooled Heavy Ion Beams in the Storage Ring ESR // Phys. Rev. Lett. 1996. V. 77. P. 3803–3815.
25. *Danared H., Kaelberg A., Simonsson A.* One-Dimensional Ordering in Coasting and Bunched Beams // J. Phys. B. 2003. V. 36. P. 1003–1010.
26. *Shirai T., Noda A., Meshkov I., Smirnov A. (Kyoto Univ.–NIRS–JINR Collab.).* One-Dimensional Beam Ordering of Protons in a Storage Ring // Phys. Rev. Lett. 2007. V. 98. P. 204801–204804.
27. *Grigorenko L. V. (for the DERICA Collab.).* DERICA Project: Dubna Electron–Radioactive Isotope Collider Facility // Phys. Part. Nucl. Lett. 2018. V. 15. P. 997–1001.
28. *Budker G. I., Dikanskii N. S., Meshkov I. N., Parkhomchuk V. V., Pestrikov D. V., Popov S. G., Skrinsky A. N.* Capabilities of Spectrometric Experiments with Hyper-Thin Internal Targets in Electron-Cooled Storage Rings of Heavy Charged Particles // Proc. of the X Intern. Conf. on High-Energy Accel., Protvino, July 1977. V. 2. P. 141–147 (in Russian).

29. *Meshkov I., Muenzenberg G., Schrieder G., Syresin E., Ter-Akopian G.* The Investigation of Nuclear Structure with Storage Rings — Present and Future // Nucl. Instr. Meth. A. 1997. V. 391. P. 2249.

30. *Ter-Akopian G. M., Greiner W., Meshkov I. N., Oganessian Yu. Ts., Reinhardt J., Trubnikov G. V.* Layout of New Experiments on the Observation of Spontaneous Electron–Positron Pair Creation in Supercritical Coulomb Fields // Intern. J. Mod. Phys. E. 2015. V. 24, No. 3. P. 1550016.

Received on July 25, 2019.